Inorganic Chemistry

Article

pubs.acs.org/IC

Bistable Dynamic Coordination Polymer Showing Reversible Structural and Functional Transformations

Sanjog S. Nagarkar,[†] Raja Das,[‡] Pankaj Poddar,[‡] and Sujit K. Ghosh*[,†]

[†]Indian Institute of Science Education and Research (IISER), Pashan, Pune, Maharashtra 411 008, India

[‡]Physical & Materials Chemistry Division, National Chemical Laboratory, Pune, Maharashtra 411 008, India.

Supporting Information

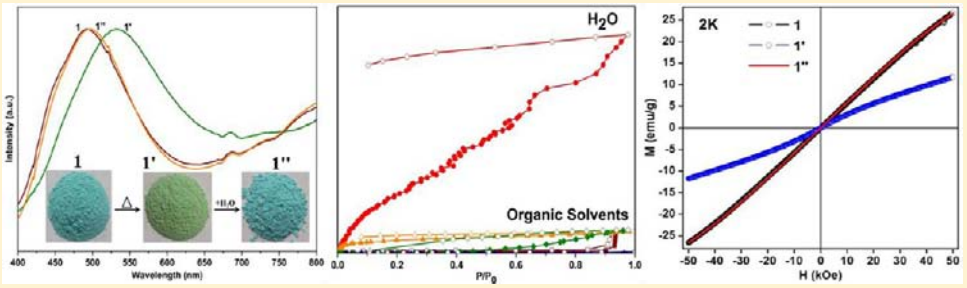

ABSTRACT: A bistable dynamic coordination polymer $[Ni(pca)(bdc)_{0.5}(H_2O)_2]$ having a two-dimensional (2D) zigzag sheet structure is synthesized solvothermally. Topological analysis revealed that the frameworks have an hcb type of uninodal net. The compound exhibits guest specific reversible structural transformations accompanying reversible changes in physical properties driven by inherent flexibility and transformability.

INTRODUCTION

Solid-state reversible structural transformations and functional studies of bistable dynamic coordination polymers (CPs) or metal−organic frameworks (MOFs) have recently attracted great attention to obtain smart functional materials.[1−15] Naturally available porous compounds like zeolites are very rigid, and soft biomolecules like enzymes are quite flexible. So, it was presumed that the rigidity and flexibility are irreconcilable and rigidity is the essential criterion to get porous materials. Generally, rigid porous structures with large surface areas are very efficient for chemical storage, but their performance for selective sorption is generally very poor. The dynamic frameworks have a blend of both rigidity and flexibility. Rigidity makes material efficient in storage and flexibility in selective sorption. Kitawaga et al. classified these dynamic frameworks as "third generation coordination polymers", also called "soft porous crystals".[1b,c]

The bistable dynamic frameworks exhibit solid-state structural transformations with breaking, making, or rearrangement of bonds driven by external stimuli like heat, light, pressure, etc.[1b,16] Structural transformations are generally accompanied by removal or exchange of guest, changes in coordination number of metal containing nodes, and conformational changes in flexible parts of organic ligands.[17] However, reports of such bistable dynamic MOFs are very few due to the difficulties in characterizing those drastic solid-state structural transformations. Generally, such structural changes in response to external stimuli are facilitated by weak bonding interactions like hydrogen-bonding and $\pi-\pi$ and C−H···π interactions. These structural transformation induced chemical and/or physical processes are much more complicated than encountered in the rigid frameworks. These materials offer unique properties such as selective and hysteretic sorption, gate opening behavior, molecular recognition, and magnetic bistability.[1b,18] Especially, magnetic bistability is very important and recently attracted great attention to the MOF community. In many cases during desolvation and resolvation processes compounds exhibit reversible changes of their magnetic properties due to loss or gain of solvent molecules, known as solvatomagnetic effect.[19] Thus, investigation of solid-state structural transformations between bistable phases and their correlation with the properties is very crucial to design smart functional materials. Herein, we report the synthesis of $[Ni(pca)(bdc)_{0.5}(H_2O)_2]$ (**1**) based coordination polymer and its dynamic behavior. The reversible solid-state structural transformations were accompanied by distinct color change on de/rehydration. The selective sorption properties were observed for adsorbates like H_2O over MeOH, EtOH, THF, toluene, etc. The dynamic and static magnetic measurements of compound **1** and those of the de/rehydrated forms were performed to trace the possible reversible structural and magnetic changes.

EXPERIMENTAL SECTION

Materials and Measurements. All the reagents and solvents were commercially available and used without further purification. FT-IR spectra were recorded on a Nicolet 6700 FT-IR spectrophotometer

Received: April 26, 2012
Published: July 24, 2012

   dx.doi.org/10.1021/ic301481p | *Inorg. Chem.* 2012, 51, 8317−8321

using KBr pellets (400−4000 cm^{-1}), X-ray powder patterns were measured on a Bruker D8 advanced X-ray diffractometer at room temperature using Cu Kα radiation (λ = 1.5406 Å) at a scan rate of 0.4 s/step and step size of 0.01° in 2θ, and thermogravimetric analyses were recorded on a Perkin-Elmer STA 6000 TGA analyzer under N_2 atmosphere with heating rate of 10 °C/min.

Synthesis. A single crystal of **1** was prepared by reacting 1 mmol of $Ni(NO_3)_2{\cdot}4H_2O$, 1 mmol of pyrazine carboxylic acid (pcaH), 0.5 mmol of 1,4-benzene dicarboxylic acid ($bdcH_2$), and 1 mmol of NaOH in 6 mL of H_2O by the solvothermal technique, in a Teflon-lined autoclave. The autoclave was heated under autogenous pressure to 160 °C for 3 days and then cooled to RT over a 24 h period. Upon cooling to RT, the desired greenish-blue crystals were obtained in ∼60% yield.

Dehydration (1′). Single crystals of **1** were heated at 140 °C under reduced pressure for 8 h, and the green dehydrated crystals were obtained.

Rehydration (1″). The dehydrated sample was taken in a glass vial and kept in a slightly bigger screw cap bottle containing water and sealed. After being stored for 3 days at room temperature, the rehydrated phase was obtained. Rehydrated phase was also obtained by keeping the dehydrated sample exposed to air, but the complete rehydration takes a long time (∼30 days).

X-ray Structural Studies. Single-crystal X-ray data on **1** were collected at 200 K on a Bruker KAPPA APEX II CCD Duo diffractometer (operated at 1500 W power: 50 kV, 30 mA) using graphite-monochromated Mo Kα radiation (λ = 0.710 73 Å). The crystal was on nylon CryoLoops (Hampton Research) with Paraton-N (Hampton Research). The data integration and reduction were processed with SAINT[20] software. A multiscan absorption correction was applied to the collected reflections. The structure was solved by the direct method using SHELXTL[21] and was refined on F^2 by full-matrix least-squares technique using the SHELXL-97[22] program package within the WINGX[23] program. All non-hydrogen atoms were refined anisotropically. All hydrogen atoms were located in successive difference Fourier maps, and they were treated as riding atoms using SHELXL default parameters. The structures were examined using the *Adsym* subroutine of PLATON[24] to ensure that no additional symmetry could be applied to the models.

Low Pressure Sorption Measurements. Low pressure gas and solvent sorption measurements were performed using BelSorpmax (Bel Japan). All of the gases/solvents used were of 99.999% purity. To obtain a guest free sample, **1** was heated under vacuum for 12 h. Prior to adsorption measurement the guest free sample **1** was pretreated at 120 °C under vacuum for 5 h using BelPrepvacII and purged with N_2 on cooling. Between the experiments with various gases, the outgassing procedure was repeated for ca. 5 h. The CO_2 sorption isotherm was measured at 195 K, and H_2O, MeOH, EtOH, THF, and toluene sorption isotherms were monitored at 298 K.

RESULTS AND DISCUSSION

Compound **1** was obtained by solvothermal reaction of pyrazine carboxylic acid (pcaH), 1,4-benzene dicarboxylic acid ($bdcH_2$), NaOH, and $Ni(NO_3)_2$ in H_2O at 160 °C. The reaction with Ni(II) yielded block-shaped greenish-blue crystals which are characterized by single crystal X-ray diffraction (SC-XRD) technique. The phase purity of the bulk material was confirmed by powder X-ray diffraction (PXRD) and thermogravimetric analysis (TGA). Compound **1** crystallizes in orthorhombic crystal system with space group *Pbca* and was formulated as $[Ni(pca)(bdc)_{0.5}(H_2O)_2]$ (Figure 1). The asymmetric unit of **1** consists of one Ni(II), one pca, half bdc, and two coordinated water molecules. Each metal ion exhibits six coordinated octahedral geometry with N_2O_4 donor set (Figure 2a). The two pyrazine rings coordinate to the metal center, and two water molecules coordinate from the side opposite to the pyrazine nitrogen's forming a 1D zigzag chain along *b* axis. These metal pyrazine 1D chains are connected at

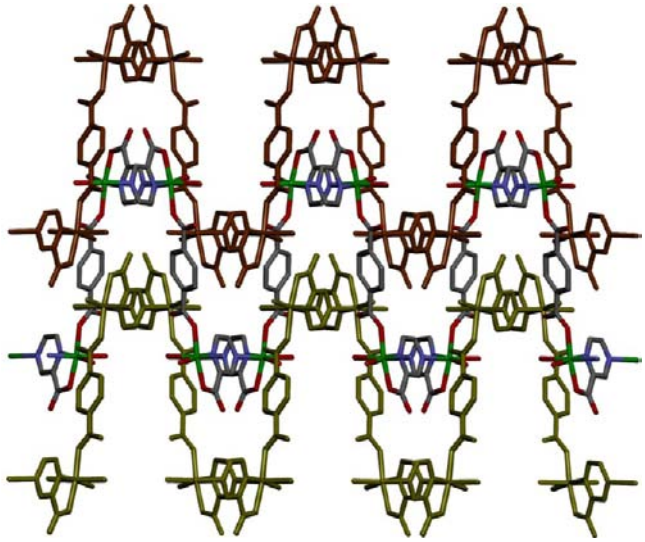

Figure 1. Arrangement of 2D sheets in compound **1** along *b* axis: metal center, green; carbon, gray; nitrogen, blue; oxygen, red. Hydrogen atoms are omitted for clarity.

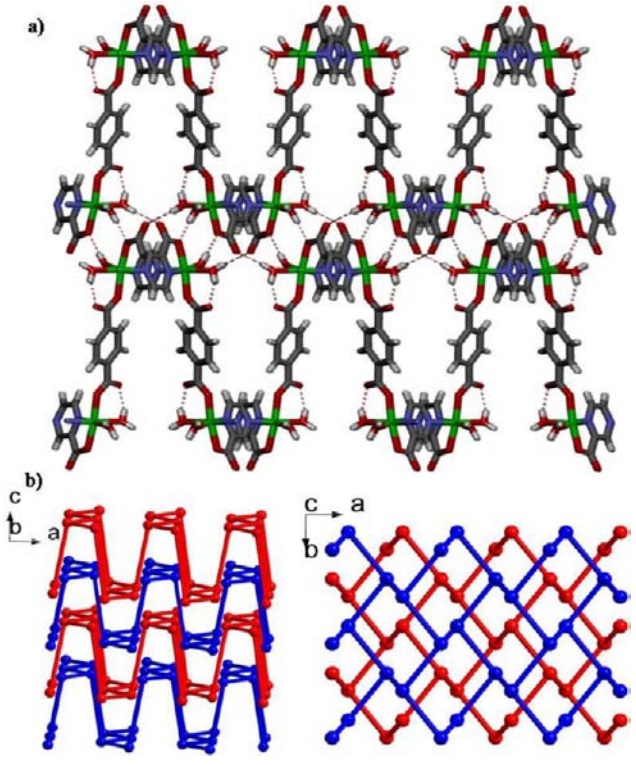

Figure 2. Hydrogen bonding between adjacent layers (A−A or B−B). (Color code: carbon, gray; nitrogen, blue; oxygen, red; nickel, green.) (b) ABAB arrangement of 2D sheets.

regular intervals by monodentate coordination of bdc carboxylate oxygen's from the side opposite to the pyrazine carboxylate, forming a 2D zigzag sheet structure. The 2D sheets are arranged one above the other in ABAB fashion (Figure 2b), and the free carboxylate oxygens from both the ligands of layer A form hydrogen bonds with the coordinated water molecules of the next A sheet present exactly above it. Similarly, the B layer is hydrogen bonded with the adjacent B sheet present above it forming hydrogen-bonded interpenetrated 3D structure.

dx.doi.org/10.1021/ic301481p | *Inorg. Chem.* 2012, 51, 8317−8321

Topological analysis using *TOPOS* software identifies the structure as having an hcb topological network, with uninodal 3-c net reported in TOPOS and RCSR TTD database,[25] which can be presented as a Schläfli symbol 6^3 (see SI for TOPOS analysis).

The thermal analysis showed that the compound is stable up to 160 °C with negligible weight loss and then ∼12.5% weight loss in the range 160−230 °C. This weight loss in the range 160−230 °C is attributed to two coordinated water molecules. After losing the coordinated water molecules, the compound forms a stable dehydrated phase which decomposes at ∼360 °C (Figure 3a). The as-synthesized compound was heated at 140

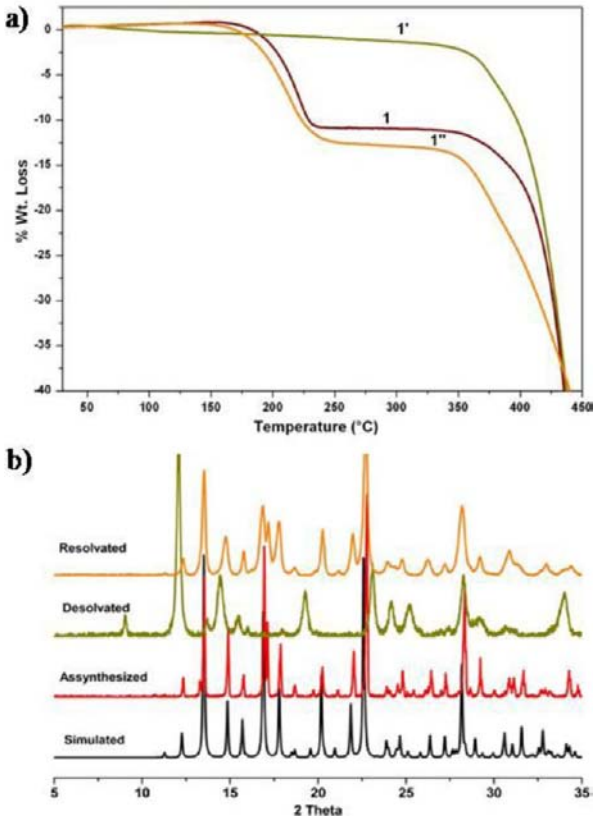

Figure 3. (a) Thermogravimetric analysis of compound **1**. (b) Powder X-ray diffraction patterns of compound **1**.

°C under reduced pressure to get the dehydrated phase, which was confirmed from TGA analysis. The PXRD pattern of dehydrated phase (**1′**) indicates that after losing coordinated water molecules the compound transforms to a new structure. This dehydrated phase (**1′**), when exposed to water vapor, again transformed back to as-synthesized structure (Figure 3b).

To understand these solid-state reversible structural transformations a single crystal was heated in situ in the SC-XRD instrument, but unfortunately at high temperature (>180 °C) the compound did not retain its single crystallanity. Thus, to trace the possible structural changes that occurred on dehydration, IR spectra of the as-synthesized, dehydrated, rehydrated compounds and the individual ligands were recorded (Figure 4a). Both as-synthesized and rehydrated compounds have a peak around 3110 cm^{-1} (m), corresponding to a water molecule,[26] but this peak is absent in the dehydrated phase indicating loss of coordinated water molecules. The peaks at 1648 cm^{-1} (s) and 1596 cm^{-1} (w) (C═O

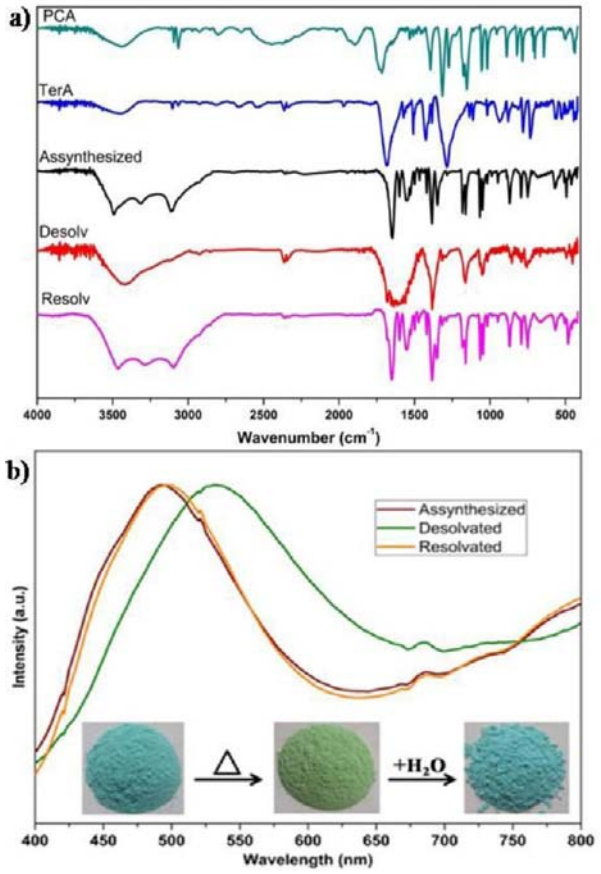

Figure 4. (a) Infrared spectrum of compound **1**. (b) Solid-state UV spectrum of compounds **1**, **1′**, and **1″**. Inset shows reversible visible color changes in compound.

carboxylate) in the as-synthesized compound are indicative of monodentate coordination of carboxylate. These peaks become broad in the case of the dehydrated compound, indicating change in the coordination environment around metal center. On exposing the dehydrated phase to water these peaks can be regenerated.

The visible color changes on de/rehydration motivated us to record the solid state UV spectrum of as-synthesized, dehydrated, and rehydrated compounds (Figure 4b). Compound **1** has an absorbance maximum at 495 nm which shifts to 532 nm (**1′**) on dehydration, with visible color change from greenish-blue to green (red shift). On rehydration, green (**1′**) again transforms back to greenish-blue (**1″**) with an absorbance maximum at 495 nm indicating that the **1** (or **1″**) and **1′** can be reversibly transformed to each other by the dehydration and rehydration process.

Bistable flexible structures generally show selective sorption properties. The compound did not adsorb any gas, since the as-synthesized compound is not very porous and the desolvated compound is supposed to transform to a more dense structure. The sorption properties for different adsorbates (H_2O, CH_3OH, EtOH, THF, and toluene) having different polarity were investigated volumetrically for **1′** at 298 K (Figure 5). In the case of H_2O as a guest (kinetic diameter, 2.65 Å), the sorption profile for **1′** increases almost linearly with increasing pressure and reaches a maximum at ∼200 mL g^{-1}, indicating the uptake of two H_2O molecules per formula unit. Desorption showed large hysteresis with negligible H_2O loss with applied

dx.doi.org/10.1021/ic301481p | *Inorg. Chem.* 2012, 51, 8317−8321

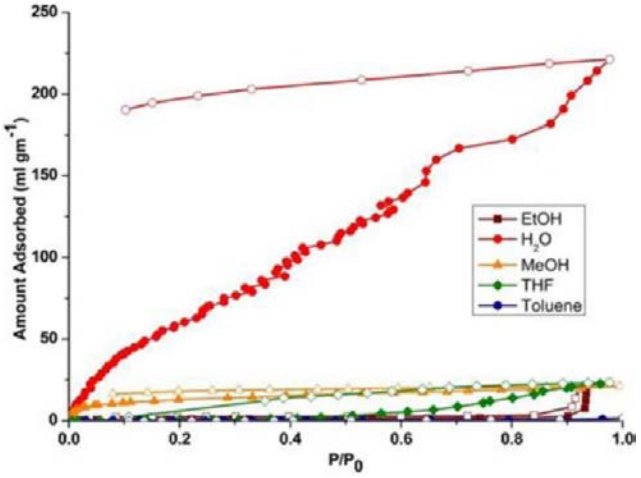

Figure 5. Adsorption isotherms for **1′** at 298 K. (Filled symbols indicate adsorption, and open symbols indicate desorption.)

vacuum. Interestingly, the sorption isotherms for CH_3OH (3.8 Å), EtOH (4.3 Å), and toluene (4.012 Å) showed negligible uptakes. The selective and slow uptake of H_2O by the dehydrated phase is ascribed to very small and polar pore windows and the H-bonding between the host and the guest, driven by inherent flexibility and transformability of the framework.[27] The selectivity was also confirmed by exposing the dehydrated phase to THF and MeOH vapors separately for 8 days. The PXRD patterns of dehydrated (**1′**) and THF or MeOH exposed (**1′**) samples were exactly the same indicating that only H_2O can transform the structure (Figure S3). These results are in agreement with the sorption isotherms of these adsorbates.

It is known that the magnetic interactions are extremely sensitive to even the smallest change in either localized or long-range structural ordering owing to their effects on the short-range direct/superexchange interactions as well as long-range dipolar interactions. The temperature dependence of magnetization in ZFC and FC mode showed the χT values for **1**, **1′**, and **1″** at 300 K are 1.1, 1.2, and 1.1 emu K mol^{-1} Oe^{-1}, respectively (Figure 6). These values are slightly higher than the spin only value of 1 emu K mol^{-1} Oe^{-1}, for one Ni (II) ion with spin value 1 and Lande *g* value 2, which could be due to a possible orbital contribution (Figures S4–S5). Upon cooling, the χT value remains almost constant down to 60 K for **1** and **1″**, whereas for **1′** it is 110 K. Below this temperature, the χT value decreases sharply to reach a minimum at 0.3, 0.23, and 0.39 emu K mol^{-1} Oe^{-1} at 2 K for **1**, **1′**, and **1″**, respectively. The sharp decrease of χT could be due to the antiferromagnetic interaction of the Ni(II) ions. Fitting of data above 80 K, with the Curie–Weiss law, gives the Curie constant C = 0.91, 0.81, and 0.87 emu K mol^{-1} Oe^{-1} and Weiss constant θ = −30, −35, and −30 K for **1**, **1′**, and **1″**, respectively. The large negative Weiss constant value indicates the presence of antiferromagnetic coupling between the Ni (II) ions. The FC and ZFC magnetization does not show irreversibility in the measured temperature range for all the samples. Below 300 K, the ZFC FC magnetization curve shows a gradual increase and changes its slope further at 80 K with no saturation effect observed until the lowest measured temperature. The ZFC and FC magnetization shows a maximum at 3 K for **1** which is a signature of antiferromagnetic interaction between the Ni(II) ions, but **1′** and **1″** do not show any maximum as **1**. The moment values for

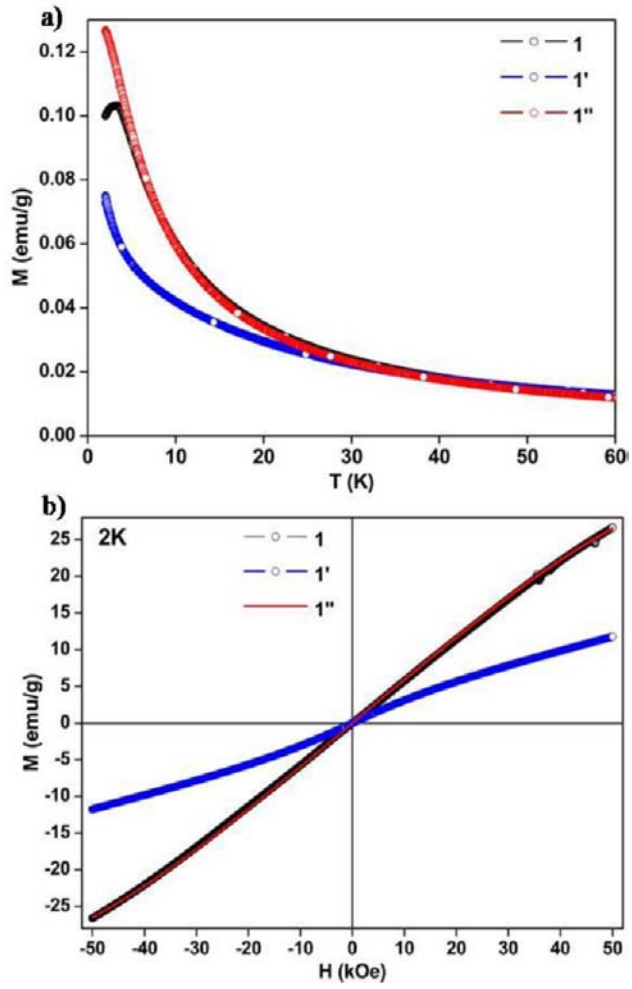

Figure 6. Temperature dependence of the magnetization at 200 Oe applied field (a) and MH loops at 2 K (b) for **1**, **1′**, and **1″**.

1 and **1″** are almost the same in the measured temperature range whereas the moment value of **1′** is lower at low temperature. After resolvation of compound **1′**, the structure of the compound changed to a very similar structure of compound **1**. This difference in magnetic moment values for **1** and **1″** is probably due to little structural damage during the dehydration and rehydration processes, which is very common for MOF compounds.

In conclusion, we have successfully synthesized a 2D coordination polymer exhibiting reversible structural transformations accompanying visible color change. The compound shows selective uptake of H_2O over other organic solvents, which is attributed to very strong affinity of polar solvent to the metal ions and the H-bonding interaction between the host and guest. The magnetic measurements showed the presence of antiferromagnetic interaction in all three compounds. The present study provides an insight into the reversible dynamic structural transformations between the two states driven by inherent flexibility and transformability, the characteristic features of multifunctional materials.

dx.doi.org/10.1021/ic301481p | *Inorg. Chem.* 2012, 51, 8317–8321

■ ASSOCIATED CONTENT

Supporting Information

Details of X-ray crystallographic data, including data in CIF format. Topology analysis for **1**. This material is available free of charge via the Internet at http://pubs.acs.org.

■ AUTHOR INFORMATION

Corresponding Author

*E-mail: sghosh@iiserpune.ac.in. Phone: +91-20-2590 8076. Fax: +91-20-2590 8186.

Notes

The authors declare no competing financial interest.

■ ACKNOWLEDGMENTS

We thank IISER Pune and Director Professor K. N. Ganesh for financial support and encouragement. S.K.G. is grateful to DAE (Project 2011/20/37C/06/BRNS) for financial support.

■ REFERENCES

(1) (a) Kitaura, R.; Noro, S.; Kitagawa, S. *Angew. Chem., Int. Ed.* **2004**, *43*, 2334. (b) Horike, S.; Shimomura, S.; Kitagawa, S. *Nat. Chem.* **2009**, *1*, 695.

(2) (a) Dinca, M.; Long, J. R. *Angew. Chem., Int. Ed.* **2008**, *47*, 2. (b) Vittal, J. J. *Coord. Chem. Rev.* **2007**, *251*, 1781.

(3) (a) Ferrey, G.; Serre, C. *Chem. Soc. Rev.* **2009**, *251*, 1380. (b) Eddaoudi, M.; Kim, J.; Rosi, N. L.; Vodak, D. T.; Wachter, J. O,; Keeffe, M.; Yaghi, O. M. *Science* **2002**, *295*, 469.

(4) (a) Bradshaw, J.; Claridhe, J. B.; Cussen, E. J.; Prior, T. J.; Rosseinsky, M. J. *Acc. Chem. Res.* **2005**, *38*, 273. (b) Lee, Y. E.; Jang, S. Y.; Suh, P. M. *J. Am. Chem. Soc.* **2005**, *127*, 6374.

(5) (a) An, J.; Shade, C. M.; C-Czegan, D. A.; Petoud, S.; Rosi, N. L. *J. Am. Chem. Soc.* **2011**, *113*, 1220. (b) Ma, S.; Zapata, F.; Lobkovsky, E. B.; Yang, J.; Chen, B. *Inorg. Chem.* **2006**, *45*, 5718.

(6) (a) Aijaz, A.; Lama, P.; Bharadwaj, P. K. *Inorg. Chem.* **2010**, *49*, 5883. (b) Kitagawa, S.; Uemura, K. *Chem. Soc. Rev.* **2005**, *34*, 109.

(7) (a) Nagarkar, S. S.; Chaudhari, A. K.; Ghosh, S. K. *Inorg. Chem.* **2012**, *51*, 572. (b) Nagarkar, S. S.; Chaudhari, A. K.; Ghosh, S. K. *Cryst. Growth Des.* **2012**, *12*, 572. (c) Joarder, B.; Chaudhari, A. K.; Ghosh, S. K. *Inorg. Chem.* **2012**, *51*, 4644.

(8) (a) Ghosh, S. K.; Kitagawa, S. *CrystEngComm* **2008**, *10*, 1739. (b) Ghosh, S. K.; Zhang, J.-P.; Kitagawa, S. *Angew. Chem., Int. Ed.* **2007**, *46*, 7965.

(9) (a) Ghosh, S. K.; Bureekaew, S.; Kitagawa, S. *Angew. Chem., Int. Ed.* **2008**, *47*, 3403. (b) Zhang, J.-P.; Ghosh, S. K.; Kitagawa, S. *Inorg. Chem.* **2009**, *48*, 7970.

(10) (a) Ghosh, S. K.; Azhakar, R.; Kitagawa, S. *Chem.—Asian J.* **2009**, *4*, 870. (b) Ghosh, S. K.; Kaneko, W.; Kiriya, D.; Obha, M.; Kitagawa, S. *Angew. Chem., Int. Ed.* **2008**, *47*, 8843.

(11) Hanson, K.; Calin, N.; Bugaris, D.; Scancella, M.; Sevov, S. C. *J. Am. Chem. Soc.* **2004**, *126*, 10502.

(12) (a) Serre, C.; Mellot-Draznieks, C.; Surble, S.; Audebrand, N.; Filinchuk, Y.; Ferey, G. *Science* **2007**, *315*, 1828. (b) Kubota, Y.; Takata, M.; Matsuda, R.; Kitaura, R.; Kitagawa, S.; Kobayashi, T. C. *Angew. Chem.* **2006**, *118*, 5054; *Angew. Chem., Int. Ed.* **2006**, *45*, 4932.

(13) Maji, T. K.; Mastuda, R.; Kitagawa, S. *Nat. Mater.* **2007**, *6*, 142.

(14) Matsuda, R.; Kitaura, R.; Kitagawa, S.; Kubota, Y.; Belosludov, R. V.; Kobayashi, T. C.; Sakamoto, H.; Chiba, T.; Takata, M.; Kawazoe, Y.; Mita, Y. *Nature* **2005**, *436*, 238.

(15) (a) Jiang, J.-J.; Li, L.; Lan, M.-H.; Pan, M.; Eichhofer, A.; Fenske, D.; Su, C.-Y. *Chem.—Eur. J.* **2010**, *16*, 1841. (b) Frey, G.; Mellot-Draznieks, C.; Serre, C.; Millange, F.; Dutour, J.; Surble, S.; Margiolaki, I. *Science* **2005**, *309*, 2040.

(16) (a) Pretsch, T.; Chapman, K. W.; Halder, G. J.; Kepert, C. J. *Chem. Commun.* **2006**, 1857. (b) Bernini, M. C.; Gandara, F.; Iglesias, M.; Snejko, N.; Gutierrez-Puebla, E.; Brusau, E. V.; Narda, G. E.; Monge, M. A. *Chem.—Eur. J.* **2009**, *15*, 4896.

(17) (a) Ghosh, S. K.; Bureekaew, S.; Kitagawa, S. *Angew. Chem., Int. Ed.* **2008**, *47*, 3403. (b) Bao, X.; Guo, P.; Liu, J.; Leng, J.; Tong, M. *Chem.—Eur. J.* **2011**, *17*, 2335.

(18) Cheng, X.-N.; Zhang, W.-X.; Lin, Y.-Y.; Zheng, Y.-Z.; Chen, X.-M. *Adv. Mater.* **2007**, *19*, 1494.

(19) Ferrando-Soria, J.; Ruiz-Garcia, R.; Cano, J.; Stiriba, S.; Vallejo, J.; Castro, I.; Julve, M.; Lloret, F.; Amoro, P.; Pasan, J.; Piuz-Perez, C.; Journaux, Y.; Pardo, E. *Chem.—Eur. J.* **2012**, *18*, 1608.

(20) *SAINTPlus (Version 7.03)*; Bruker AXS Inc.: Madison, WI, 2004.

(21) Sheldrick, G. M. *SHELXTL, Reference Manual, Version 5.1*; Bruker AXS: Madison, WI, 1997.

(22) Sheldrick, G. M. *Acta Crystallogr., Sect. A* **2008**, 112.

(23) Farrugia, L. J.*WINGX version 1.80.05*; University of Glasgow: Glasgow, 2009.

(24) Spek, A. L. *PLATON, A Multipurpose Crystallographic Tool*; Utrecht University: Utrecht, The Netherlands, 2005.

(25) Blatov, A. V.; Proserpio, D. M. *Acta Crystallogr.* **2009**, *A65*, 202.

(26) Kanoo, P.; Ghosh, A. C.; Cyriac, S. T.; Maji, T. K. *Chem.—Eur. J.* **2012**, *18*, 237.

(27) (a) Kanoo, P.; Sambhu, R.; Maji, T. K. *Inorg. Chem.* **2011**, *50*, 400. (b) Hijikata, Y.; Horike, S.; Sugimoto, M.; Sato, H.; Mastuda, R.; Kitagawa, S. *Chem.—Eur. J.* **2011**, *17*, 5138.